Journal of Applied Polymer Science

Preparation and properties of octadecylamine modified graphene oxide/styrene-butadiene rubber composites through an improved melt compounding method

Chunwei Wang, Zijin Liu, Shifeng Wang, Yong Zhang
State Key Laboratory of Metal Matrix Composites, School of Chemistry and Chemical Engineering, Shanghai Jiao Tong University, Shanghai 200240, China
Correspondence to: Y. Zhang (E-mail: yong_zhang@sjtu.edu.cn)

ABSTRACT: Octadecylamine modified graphene oxide/styrene-butadiene rubber (GO-ODA/SBR) composites are prepared by a novel and environmental-friendly method called "Improved melt compounding". A GO-ODA/ethanol paste mixture is prepared firstly, and then blended with SBR by melt compounding. GO-ODA sheets are uniformly dispersed in SBR as confirmed by scanning electron microscope, transmission electron microscopy, and X-ray diffraction. The interfacial interaction between GO-ODA and SBR is weaker than that between GO and SBR, which is proved by equilibrium swelling test and dynamic mechanical analysis. GO-ODA/SBR show more pronounced "Payne effect" than GO/SBR composites, indicating enhanced filler networks resulted from the modification of GO with ODA. GO-ODA/SBR composite has higher tensile strength and elongation at break than SBR and GO/SBR composite. The tensile strength and elongation at break for the composite with 5 parts GO-ODA per hundred parts of rubber increase by 208% and 172% versus neat SBR, respectively. © 2015 Wiley Periodicals, Inc. J. Appl. Polym. Sci. **2016**, *133*, 42907.

KEYWORDS: composites; graphene and fullerenes; glass transition; mechanical properties; nanotubes; rubber

Received 17 July 2015; accepted 4 September 2015
DOI: 10.1002/app.42907

INTRODUCTION

Graphene/polymer composites have attracted great attention owing to their outstanding properties.[1,2] But, graphene is not always the best choice due to its high manufacturing cost, difficulty for dispersion into polymer and lack of functional groups for bonding with polymers. As a precursor of graphene in the Hummers method, graphene oxide (GO) has abundant reactive oxygen-containing groups and can be well dispersed in water,[3,4] and its polymer composites have also been paid much attention from the point view of commercial application.[5–9]

Dispersion state and interfacial interaction between GO and polymers are two key factors affecting the properties of GO/polymer composites. The dispersion state strongly depends on mixing methods. Basically, there are three kinds of methods to prepare GO/polymer composites in polymer processing: melt compounding,[10] solution mixing,[11] and latex compounding.[12] Melt compounding is the most simple and suitable method for industrial production, but its main disadvantage is the poor dispersion of GO in polymers. Solution mixing leads to well dispersion, but the removal of solvents is an environmental issue. Latex compounding can get well dispersion of GO in a polymers, but its prerequisite is that the polymer exists in latex, and only limited polymers meet this prerequisite. It is important to explore a new method that can overcome the disadvantages mentioned above without compromising the need of well dispersion for preparing GO/polymer composites.

Because GO is a hydrophilic filler, the poor dispersion and weak load transfer are two disadvantages of its composites with nonpolar rubbers such as polybutadiene (BR) and styrene-butadiene rubber (SBR), and modification of GO is often needed. Octadecylamine (ODA) can be used to functionalize GO for the well dispersion of GO in rubbers. ODA modification of GO could improve its exfoliation in BR composites prepared by solution mixing, leading to better toughness and elongation at break.[13] GO/SBR composites were prepared through latex co-coagulation and *in situ* modification with oleylamine or ODA, and the modification led to better reinforcing efficiency.[14] Considering the effective modification of GO with ODA, we think it is crucial to investigate the interfacial interaction between GO and rubbers like SBR. How will the interfacial interaction between GO and SBR after GO is modified with ODA?

In previous studies, functionalized GO/polymer composites were mainly prepared by solution mixing method, which

involved using large quantities of toxic solvents. In this work, we explored a novel and environmentally friendly method based on the melt compounding to prepare ODA modified GO (GO-ODA)/SBR composites.[15] This method was named as "Improved melt compounding" method. A small amount of nontoxic solvent ethanol was used to assist the dispersion of GO-ODA, followed by the traditional melt compounding. The dispersion of GO-ODA in SBR, the interfacial interaction between GO and SBR before and after modified with ODA and the mechanical properties of the composites were investigated.

EXPERIMENTAL

Materials

Flake graphite (99.8%) with average particle size of 45 μm was purchased from Alfa Aesar company. Octadecylamine (90%) was purchased from Sigma Aldrich Company. Styrene-butadiene rubber (SBR1500) with styrene content of 23.5% was produced by Qilu Petroleum Co., China. The chemicals including ethanol, $KMnO_4$, concentrated H_2SO_4, concentrated HCl, 30% H_2O_2 aqueous solution, and dicumyl peroxide (DCP) were all analytical grade and purchased from Sinopharm Chemical Reagent, China.

Preparation of GO-ODA

Graphite oxide was prepared through a modified Hummers method from flake graphite.[16] GO was produced by exfoliation of the graphite oxide. Graphite oxide was dispersed in water (1 mg/ml), treated in an ultrasonic bath and stirred for 4 h. Then GO power was obtained by freeze-drying. For preparing GO-ODA, the GO suspension under ultra-sonication was mixed with an ODA/ethanol (10 mg/mL) solution at a GO/ODA weight ratio of 2/3, followed by refluxing at 90°C for 24 h. Then, GO-ODA was purified by washing with warm ethanol for at least five times to remove residual ODA, and then dried in an oven at 80°C for 24 h.

Preparation of GO-ODA/SBR Composites

GO-ODA/SBR composites were prepared by the "Improved melt compounding" method. GO-ODA was dispersed in ethanol at a concentration of 10 mg/mL by ultra-sonication, and then the ethanol was evaporated to obtain a GO-ODA/ethanol paste which had a small amount of ethanol. The paste was mixed with SBR in the mixing chamber of Haake rheomerter at a rotor speed of 60 rpm for 20 min. The mixing temperature was set at 80°C so that the ethanol in the paste could evaporate while GO-ODA was dispersed into SBR. The resultant composite was mixed with DCP on a two-roll mill and compression molded at 170°C for the optimum vulcanization time.[17] For comparison, GO/SBR composites were prepared by using the same procedure. The formulations for GO (GO-ODA)/SBR composites are as follows: SBR 100, DCP 0.4, GO 0-3, GO-ODA 0-5 phr (parts per hundred parts of rubber). The procedure for preparing GO-ODA and SBR composites is given in Figure 1.

Characterizations

Atomic Force Microscopy (AFM). AFM height images of GO and GO-ODA were taken on a Nano Scope III A (Digital Instrument, USA) in a tapping mode. GO and GO-ODA with a concentration of 0.0025 mg/mL were well dispersed in deionized water and ethanol, respectively, and then spin-coated on mica substrates and dried under room temperature for AFM observation.

Fourier Transform Infrared Spectroscopy (FTIR). FTIR spectra were recorded using a Spectrum 100 (Perkin Elmer, USA) to characterize the chemical structure of ODA, GO and GO-ODA. The tests were carried out at a resolution of 4 cm^{-1} in a wave number range of 4000 to 400 cm^{-1} using attenuated total reflectance mode.

X-ray Diffraction (XRD). XRD spectra were recorded by D-MAX 2200/PC, (Japan Rigaku Corporation) with Cu Kα radiation source at a wavelength of 1.54 Å.

Thermogravimetric Analysis. TGA was performed on a Q5000IR (TA Instruments, USA) under a nitrogen flow of 40 mL/min from room temperature to 700°C at a heating rate of 20°C/min.

Scanning Electron Microscopy (SEM). SEM micrographs of GO (GO-ODA)/SBR composites were taken by a field-emission scanning electron microscopy (Nova Nano SEM NPE218, Japan). Cryogenic fracture surfaces of the specimens were coated with gold by sputtering before observation.

Transmission Electron Microscopy (TEM). TEM micrographs of GO (GO-ODA)/SBR composites were taken by a 120 kV biology transmission electron microscopy (Tecnai G2 spirit Biotwin, USA). The Ultrathin specimens were cryogenically cut with a diamond knife using an ultra-thin microtome (Leica UC6, Germany).

Equilibrium Swelling Test. SBR vulcanizate samples were swollen in toluene at 25°C for 72 h to achieve equilibrium swelling. The weights of the samples before and after swelling were recorded. Then the samples were dried in a vacuum oven at 80°C for 48 h to remove all the solvent, and weighed again.

Glass Transition Temperatures (T_g). T_g of the samples were measured on a dynamic mechanical analyzer (DMA) Q8000 (Perkin Elmer, USA), using a frequency of 1 Hz from −80 to 20°C, with a tensile mode at a heating rate of 3°C/min.

Payne Effect. Strain sweeps from 0.28% to 300% were performed for GO(GO-ODA)/SBR compounds on a Rubber Process Analyzer (RPA2000, Alpha Technologies, USA) at 60°C with a frequency of 1 Hz.

Tensile Test. Tensile properties of the composites were measured on a universal test machine (Instron 4465, USA) in accordance with ASTM D412-06a at a speed of 500 mm/min.

RESULTS AND DISCUSSION

AFM Analysis of GO-ODA

AFM images and the height profiles of GO and GO-ODA nanosheets are shown in Figure 2. The thickness of GO is about 0.8 nm, which is larger than the theoretical monolayer graphene sheet with van der Waals thickness of about 0.34 nm.[18] This is because of the presence of many oxygen-containing groups on GO. After functionalization with ODA, the thickness of GO

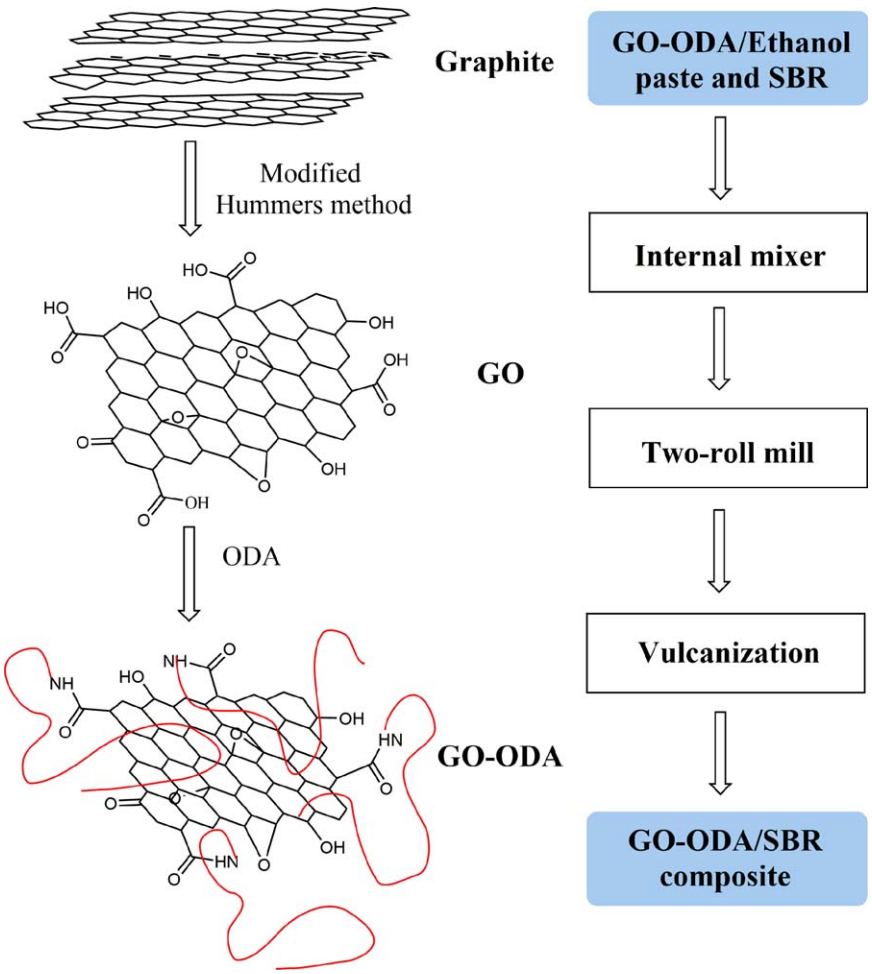

Figure 1. Schematic representation for preparation of GO-ODA and GO-ODA/SBR composites. [Color figure can be viewed in the online issue, which is available at wileyonlinelibrary.com.]

sheet increased to about 1.6 nm. This is consistent with the results that have been reported in the literatures.[19,20]

FTIR Analysis of GO-ODA

The FTIR spectra of GO, ODA, and GO-ODA are shown in Figure 3. Infrared absorption characteristic peaks of GO appear at 3434 cm^{-1} (O-H stretching from OH groups), 1718 cm^{-1}, 1400 cm^{-1}, 1228 cm^{-1}, (C═O stretching, C—O—H in-plane blending, C—O stretching from COOH groups, respectively), 1113 cm^{-1}, 1063 cm^{-1} (C—O—C stretching from epoxy groups), and 1629 cm^{-1} (aromatic C═C stretching). In the spectrum of GO-ODA, the appearance of peaks at 2918 cm^{-1}, 2850 cm^{-1}, 1470 cm^{-1}, and 720 cm^{-1} (methylene asymmetrical C—H stretching, methylene symmetrical C—H stretching, methyl asymmetrical C—H bending and methylene rocking, respectively) indicate the presence of octadecyl on GO. For the characteristic absorption of COOH, the peaks at 1718 cm^{-1} and 1228 cm^{-1} disappear and the peak at 1400 cm^{-1} becomes weaken obviously. New peaks appear at 1645 cm^{-1} and 1550 cm^{-1} (C═O stretching, N—H in-plane blending and C—N stretching from amide groups). All these results indicate that an amide reaction between COOH group on GO and amino group on ODA occurs during the functionalization step. What's more, the peak at 3335 cm^{-1} (N—H stretching of primary amine on ODA) disappears, which can also support this reaction.

XRD Analysis of GO-ODA

XRD patterns of graphite, GO, GO-ODA, and ODA are shown in Figure 4. The typical (002) diffraction peak of graphite appears at 26.4°. The diffraction peaks of GO and GO-ODA shift to 10.4° and 6.5°. According to the Bragg equation, $2d{\cdot}\sin\theta = n\lambda$ (d is interplanar spacing, θ is complementary angle of the X-ray incident angle, λ is wavelength of the X-rays, n is a positive integer), the interlayer spacings of graphite, GO and GO-ODA are calculated to be 0.34, 0.85 and 1.36 nm, respectively. Shanmugharaj *et al.*[21] considered the increased layer spacing of GO as the oxygen-containing groups. After functionalized with ODA, the interlayer spacing of GO further increases because of the attachment of ODA onto GO. Moreover, the diffraction peak of GO-ODA gets broader than that of GO or graphite, which means the GO layers of GO-ODA become more disordered along the stacking directions of GO layers and the distribution of interlayer distance between GO layers becomes broader.[22,23] The diffraction peaks of ODA do not appear on the XRD patterns of GO-ODA, which indicates that the free ODA molecules have been fully washed away.

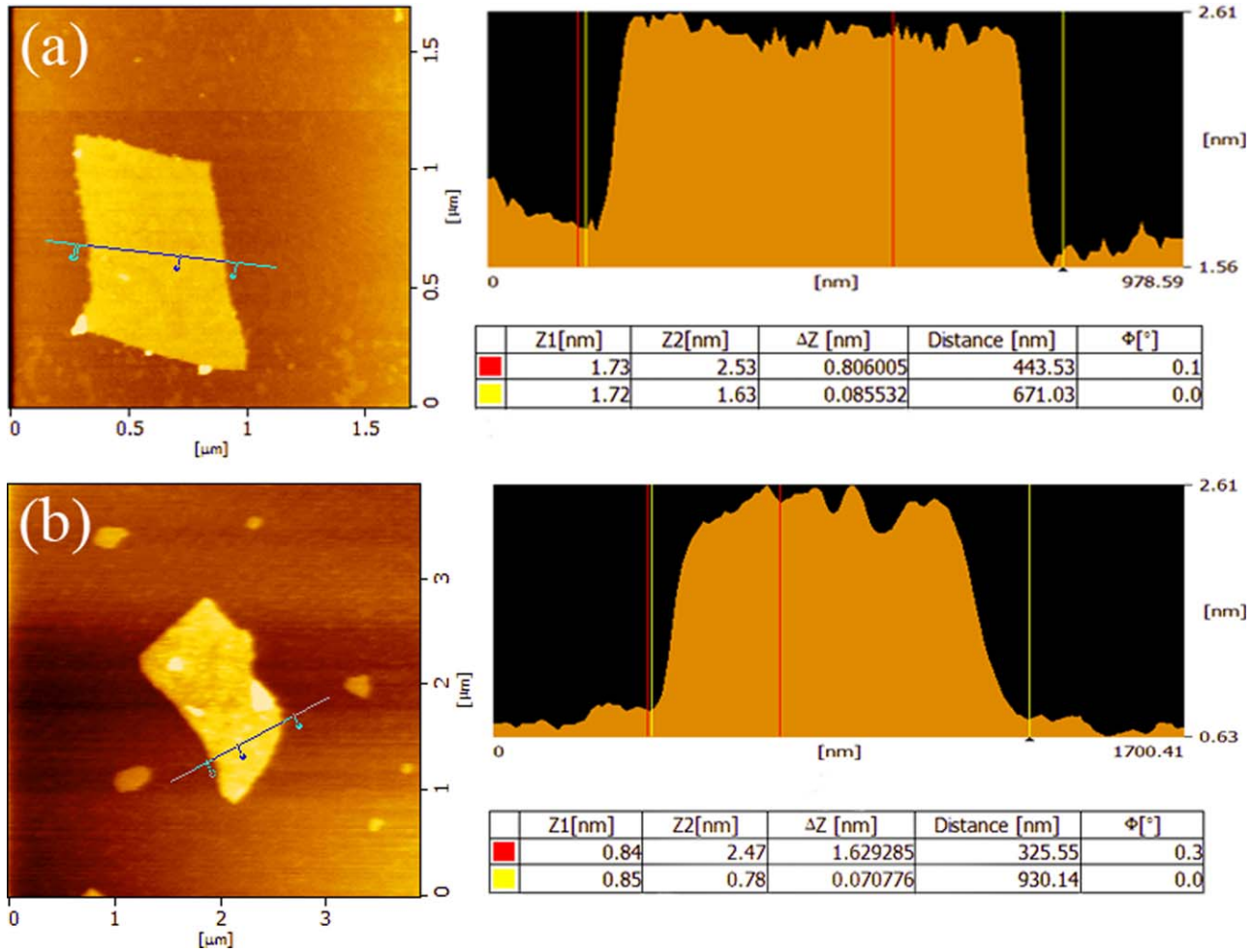

Figure 2. Tapping mode AFM images and their height profiles of GO (a) and GO-ODA (b). [Color figure can be viewed in the online issue, which is available at wileyonlinelibrary.com.]

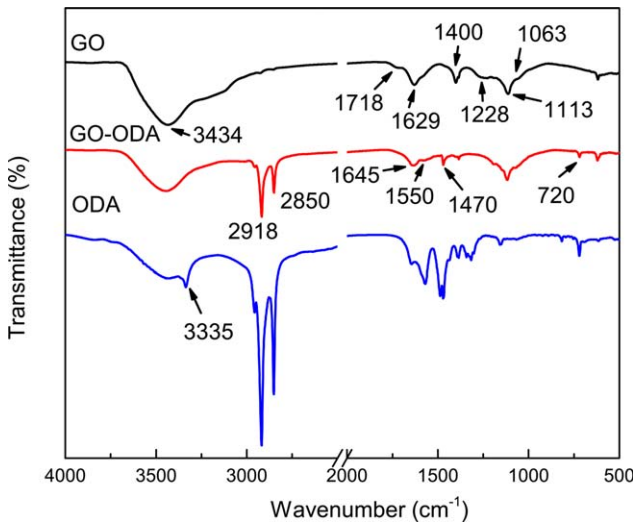

Figure 3. FTIR spectra of GO, ODA, and GO-ODA. [Color figure can be viewed in the online issue, which is available at wileyonlinelibrary.com.]

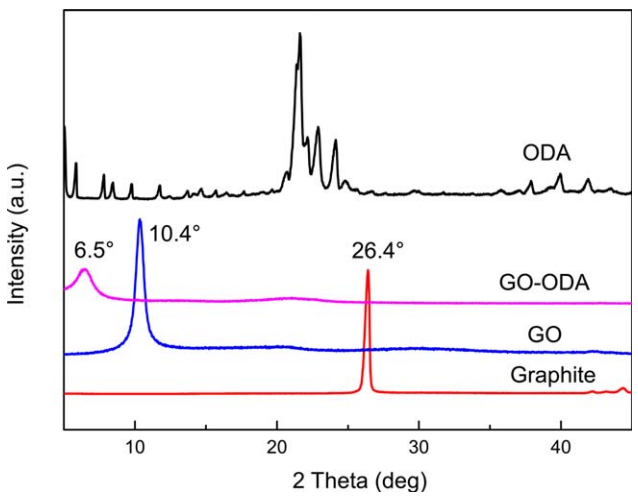

Figure 4. XRD patterns of Graphite, GO, GO-ODA, and ODA. [Color figure can be viewed in the online issue, which is available at wileyonlinelibrary.com.]

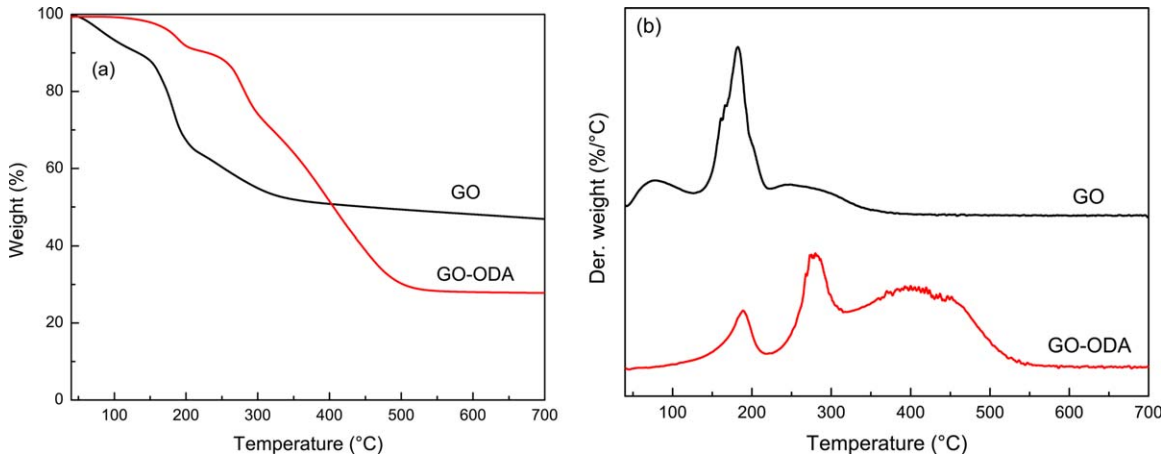

Figure 5. TGA (a) and DTG (b) curves of GO and GO-ODA in nitrogen. [Color figure can be viewed in the online issue, which is available at wileyonlinelibrary.com.]

TGA of GO-ODA

TGA is used to estimate the degree of GO functionalization with ODA. Figure 5(a) shows the TGA curves of GO and GO-ODA. The corresponding DTG curves are shown in Figure 5(b). GO shows about 8.6% weight loss at 125°C, which is caused by evaporation of absorbed water.[13] By contrast, GO-ODA is thermal stable and shows little weight loss at 125°C. These results illustrate that GO is changed from hydrophilic to hydrophobic after functionalized with ODA. For GO, about 37.4% weight loss is observed between 125°C and 380°C, which is resulted from decomposition of its oxygen-containing groups. GO-ODA shows 70.6% weight loss from 125°C to 550°C because of the decomposition of ODA molecules and the oxygen-containing groups that did not react with ODA.[24] The final amount of residual carbon of GO and GO-ODA at 700°C are 44.1% and 27.8%, respectively. Based on these results, the weight fraction of ODA on GO-ODA is calculated to be 37%.

SEM Analysis

Figure 6 show the SEM micrographs of GO (GO-ODA)/SBR composites. Bright spots are GO or GO-ODA sheets, while dark region is SBR matrix. In Figure 6(a), many bright spots with dimensions up to several microns are dispersed in SBR, and there are several holes left in the matrix which are the big agglomerates of GO that have been pulled out from SBR during brittle fracture at low temperature. This result indicates that GO sheets agglomerate together and are hard to exfoliate. By contrast, the bright spots in Figure 6(b) are much smaller in size and well dispersed in SBR matrix. Little visible large agglomerate or holes appear in the cross section, which confirms the dispersion of GO-ODA in SBR is much better than that of GO.

TEM Analysis

TEM is performed to examine the dispersion of GO and GO-ODA in SBR. In Figure 7(a), GO sheets aggregate together and are poorly dispersed in SBR over the cross section. By contrast, GO-ODA sheets show a much more uniform dispersion state over the cross section in Figure 7(b,c). It is speculated that ODA molecules hinder GO sheets from stacking, thus facilitating the dispersion of GO-ODA in SBR. Till to now, researchers have tried various methods to exfoliate GO into monolayer in the matrix, but it is still a big challenge. Araby et al.[25] investigated the effect of processing method on the dispersion of graphene plates (GnPs) in SBR, and they found GnPs showed a serious aggregation in the matrix by melt compounding method, while a better dispersion and exfoliation by solution mixing method. But it still cannot avoid GnPs stacking in the matrix. This method suggested in our work can reach the similar dispersion state of GO in rubber as obtained by solution mixing, and is more suitable for industrial production.

XRD Analysis

XRD is widely used to assess the dispersion state of plate-like fillers in polymer matrix.[26–30] Figure 8 presents XRD patterns of

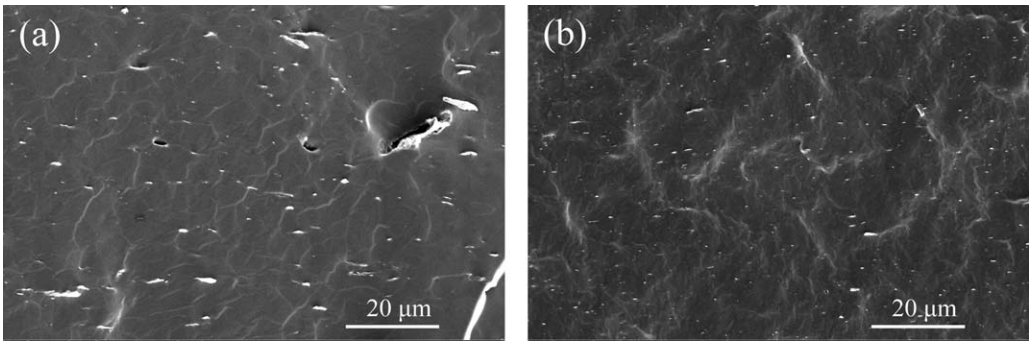

Figure 6. SEM micrographs of fracture surfaces of (a) GO/SBR (3/100) and (b) GO-ODA/SBR (3/100) composites.

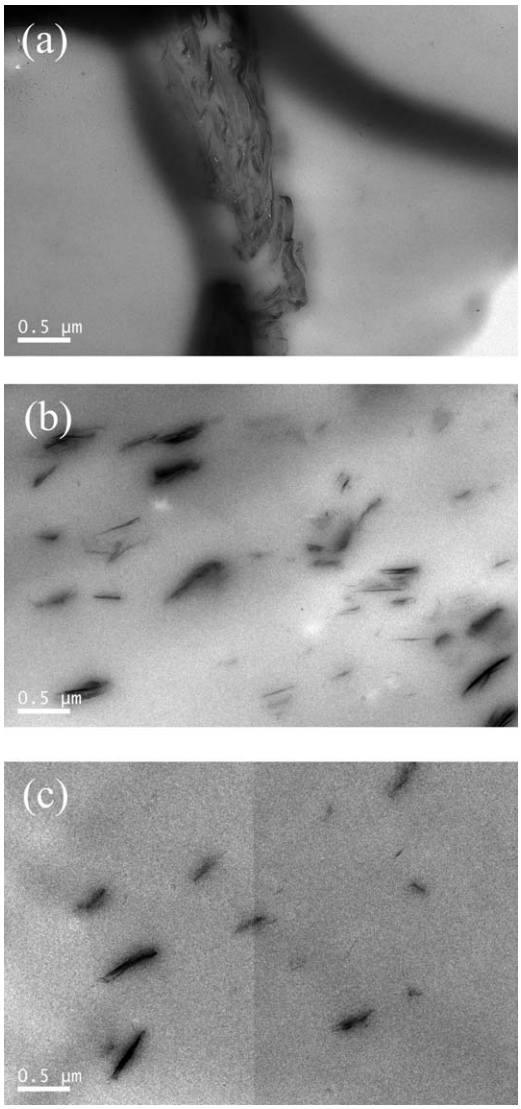

Figure 7. TEM micrographs of (a) GO/SBR (3/100), (b) GO-ODA/SBR (3/100), and (c) GO-ODA/SBR (1/100) composites.

GO-ODA/SBR composites at different GO-ODA content. For all the composites, the broad diffuse peak between 10° to 28° corresponds to the diffraction from amorphous SBR phase.[31,32] When the GO-ODA content is 2 phr or less, no diffraction peak of GO-ODA is observed, indicating that GO-ODA sheets are well dispersed in SBR matrix.[33] However, a small peak at 7.2° is observed when the GO-ODA content is 3 phr, which becomes particularly pronounced when the GO-ODA content is 5 phr, suggesting the presence of a significant concentration of multilayer tactoids.[16] This is consistent with the result observed by TEM in Figure 7(b).

Kraus Curves

Equilibrium swelling experiment is used to investigate the interaction between SBR and GO before and after modified with ODA with the help of Kraus plots. The Kraus equation is as follows:[34]

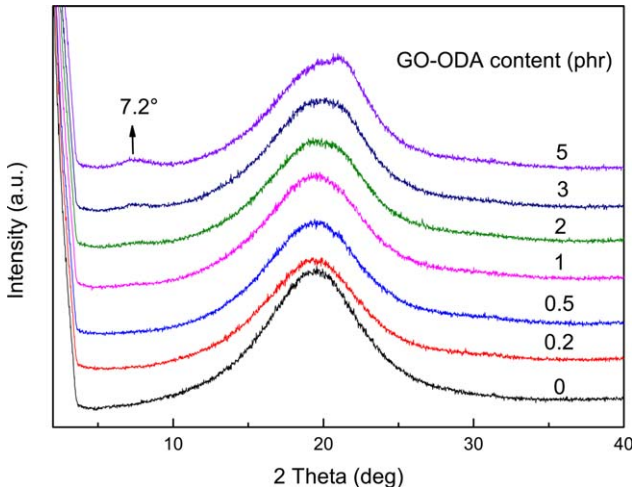

Figure 8. XRD patterns of GO-ODA/SBR (variable/100) composites. [Color figure can be viewed in the online issue, which is available at wileyonlinelibrary.com.]

$$V_{r0}/V_{rf} = 1 - m\left(\frac{f}{1-f}\right) \quad (1)$$

where, m is the rubber-filler interaction parameter, f the filler volume fraction, V_{r0} equilibrium volume fraction of the rubber in the unfilled system, and V_{rf} equilibrium volume fraction of the rubber in the filled system. V_{rf} is calculated by the following equation:

$$V_{rf} = \frac{(d - fw)\rho_p^{-1}}{(d - fw)\rho_p^{-1} + A_s\rho_s^{-1}} \quad (2)$$

where d is the dried weight of the swollen vulcanizate, f the filler volume fraction, w the initial weight of the vulcanizate, ρ_p the density of rubber, ρ_s the density of the solvent, and A_s the amount of solvent absorbed by rubber.

The dependence of V_{r0}/V_{rf} on filler content is illustrated in Figure 9 and the slope can be a measurement of polymer-filler

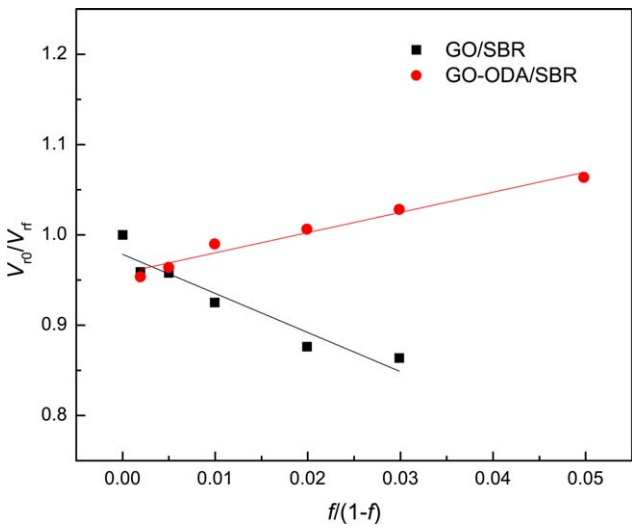

Figure 9. Kraus plots for GO (GO-ODA)/SBR composites. [Color figure can be viewed in the online issue, which is available at wileyonlinelibrary.com.]

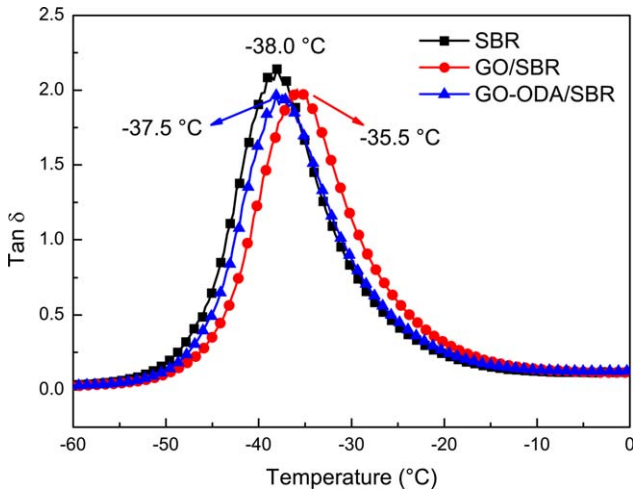

Figure 10. DMA plots of tan δ versus temperature for SBR, GO/SBR (3/100), and GO-ODA/SBR (3/100) composites. [Color figure can be viewed in the online issue, which is available at wileyonlinelibrary.com.]

interaction parameter.[35] There is a strong adhesion between a polymer and a filler if the curve of the Kraus plots is offset downward from the straight line $V_{r0}/V_{rf}=1$, and the greater deviation the stronger adhesion. Conversely, the curve of the Kraus plots deviating upward from the straight line $V_{r0}/V_{rf}=1$ means a weak adhesion between a polymer and a filler, and the greater the weaker.[36] For GO/SBR composites, the curve of the Kraus plots is downward, indicating the stronger polymer-filler interaction. However, the curve turns upward for GO-ODA/SBR composites, implying the weak polymer-filler interaction. This should be attributed to the existence of ODA molecules that work as spacers between GO and SBR, thus decreasing the interaction between GO and SBR.

Glass Transition Temperature

T_g is an effective proof to measure the polymer-filler interaction.[37,38] In Figure 10, T_g increases from −38.0°C for SBR to −35.5°C for GO/SBR composite because GO sheets restrict the segmental mobility of SBR during dynamic mechanical loading.[39] This result is an evidence of efficient interaction between GO and SBR matrix.[40] T_g of GO-ODA/SBR decreases to −37.5°C, lower than that of GO/SBR, indicating the reduced interface interaction between GO-ODA and SBR. For GO-ODA/SBR composite, T_g is affected by two factors: GO increases T_g, while the presence of ODA decreases T_g because of its spacer effect. The two factors decrease the T_g of GO-ODA/SBR composite.

Payne Effect

RPA can give detailed information about the filler network and the filler-rubber interaction in a wide range of strain amplitude (γ).[37] Figure 11 shows the γ dependence of the storage modulus (G') for SBR compounds.

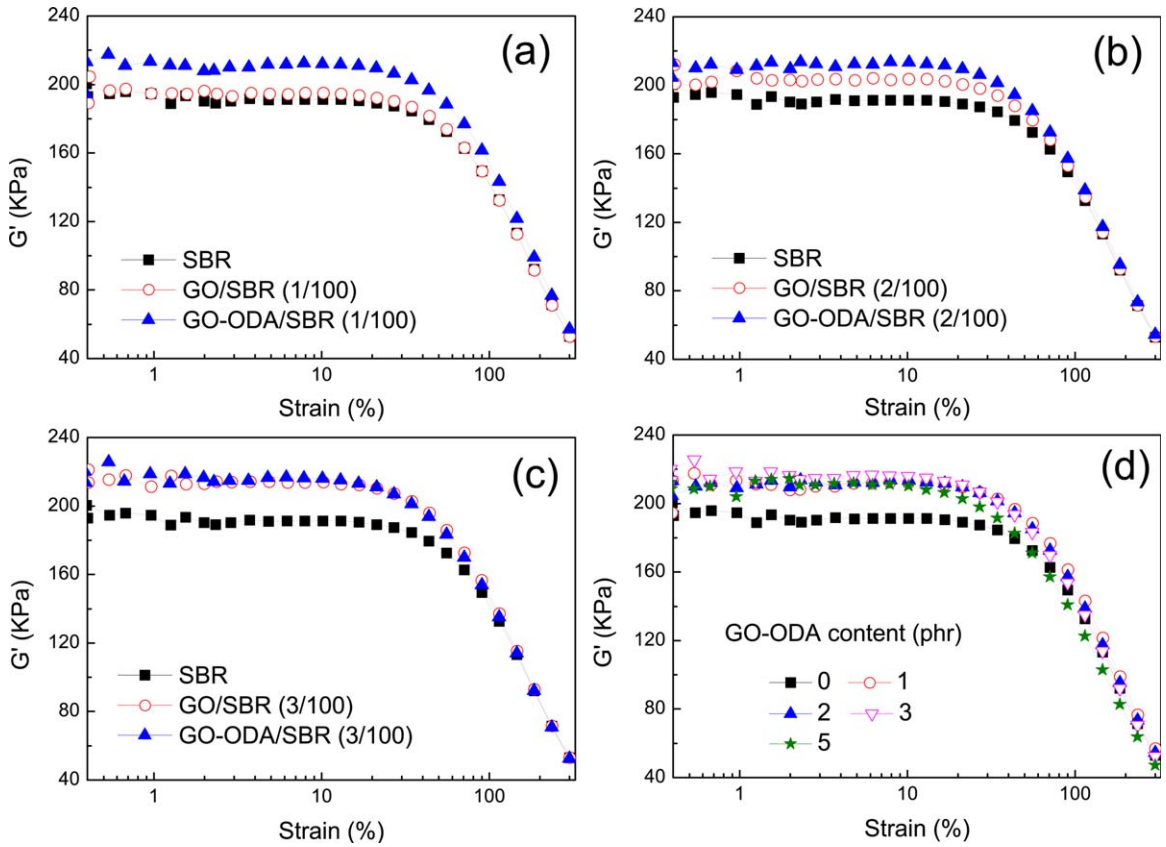

Figure 11. Comparison of storage modulus with strain amplitude for SBR compounds with the same filler content (a) 1/100, (b) 2/100, (c) 3/100, and (d) various GO-ODA content. [Color figure can be viewed in the online issue, which is available at wileyonlinelibrary.com.]

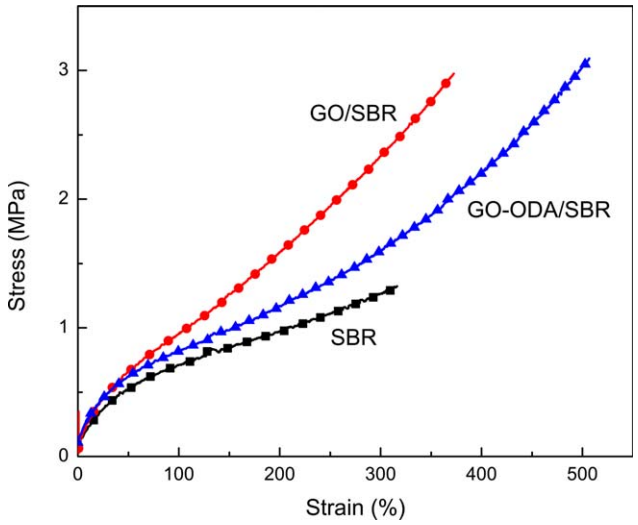

Figure 12. Stress–strain curves for SBR, GO/SBR (3/100), and GO-ODA/SBR (3/100). [Color figure can be viewed in the online issue, which is available at wileyonlinelibrary.com.]

All the compounds exhibit linear viscoelastic behavior at low γ range ($\gamma < 30\%$), and nonlinear viscoelastic behavior at high γ range. The transition point from the linear to nonlinear viscoelastic behavior is defined as critical strain (γ_c). This typical behavior is the well-known "Payne effect".[38,39] It is widely accepted that "Payne effect" is mainly due to the breakdown of filler network and thus release of the rubber trapped in the filler network.[40,41] It should be noted that a decrease of G' is also observed for neat SBR at high γ, which is related to the disentanglement of the SBR macromolecule chains.[40,42]

It can be seen from Figure 11(a–c), the G' of GO-ODA/SBR compound is higher than that of GO/SBR compound at the same filler content, especially in the linear viscoelastic region, indicating enhanced filler networks resulted from the modification of GO with ODA. Subramaniam *et al.*[41] reported a similar trend in their study on dynamic properties of ionic liquid modified multi-walled carbon nanotubes/polychloroprene rubber composites. It was considered that ionic liquid facilitated the disentanglement and dispersion state of nanotubes in rubber, leading to additional filler networks, which in turn improved the G'.

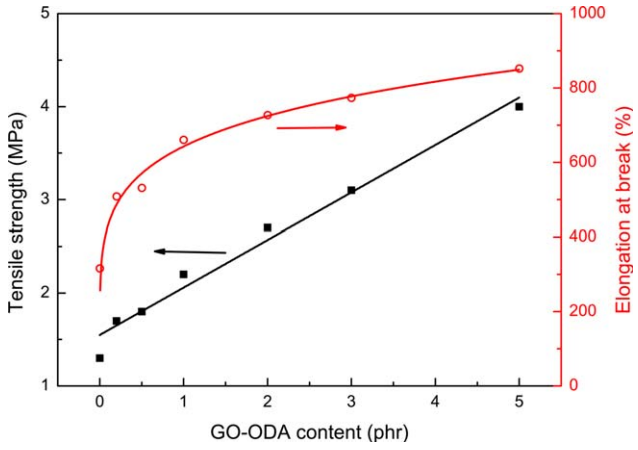

Figure 13. Variation in tensile strength and elongation at break with various GO-ODA content for GO-ODA/SBR composites. [Color figure can be viewed in the online issue, which is available at wileyonlinelibrary.com.]

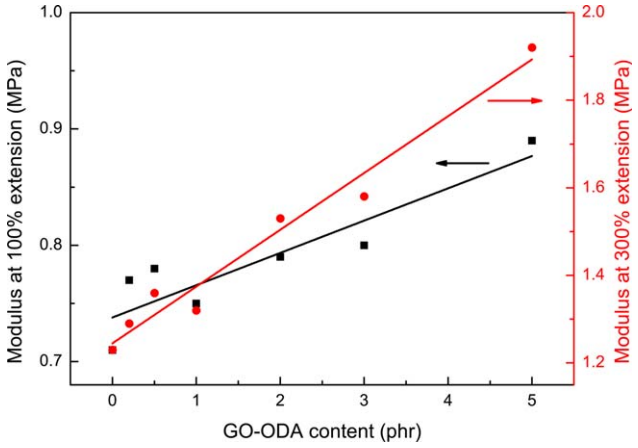

Figure 14. Variation in modulus at 100% extension and 300% extension with GO-ODA content for GO-ODA/SBR composites. [Color figure can be viewed in the online issue, which is available at wileyonlinelibrary.com.]

Figure 11(d) shows that the γ_c decreases with increasing GO-ODA content. This is attributed to the formation of weak filler networks. The weak filler networks are easy to be broken down at low γ.[43]

Mechanical Properties

Figure 12 illustrates the stress−strain behavior of SBR composites. GO/SBR and GO-ODA/SBR have higher modulus, tensile strength and elongation at break than SBR. GO-ODA/SBR has lower modulus but higher tensile strength and elongation at break than GO/SBR composite. This may be attributed to the weaker interfacial interaction between GO-ODA and SBR than that between GO and SBR. In addition, compared with 3 phr GO in GO/SBR composite, the actual GO content in GO-ODA/SBR composite is less than 3 phr because of the existence of 37% ODA functionalized onto GO, which may be another reason for lower modulus of GO-ODA/SBR than that of GO/SBR composite.

Figures 13 and 14 show the mechanical properties of GO-ODA/SBR composites with different GO-ODA content. The tensile strength, elongation at break, moduli at 100% and 300% extension increase with increasing GO-ODA content. The tensile strength and elongation at break for the composite with 5 phr GO-ODA increase by 208% and 172% versus neat SBR vulcanizate, respectively.

CONCLUSIONS

GO is successfully modified by ODA to obtain GO-ODA with ODA content of ca. 37%. The environmental-friendly "Improved melt compounding" method of mixing GO and GO-ODA pastes with SBR is suggested, and proved to be an effective method to well disperse GO sheets into SBR matrix, which opens a new approach to the large-scale production of GO-filled SBR

compounds and vulcanizates. GO modification with ODA can improve the dispersion of GO in SBR, and decrease the interfacial interaction between GO and SBR as proved by Kraus curves and decrease modulus at a given extension of GO-ODA/SBR. GO-ODA/SBR show more pronounced "Payne effect" than GO/SBR composites as evidenced by a Rubber Process Analyzer, indicating enhanced filler networks resulted from the modification of GO with ODA. The tensile strength, elongation at break, moduli at 100% and 300% extension of GO-ODA/SBR increase with increasing GO-ODA content. The tensile strength and elongation at break for the composite with 5 phr GO-ODA increase by 208% and 172% versus neat SBR vulcanizate, respectively.

ACKNOWLEDGMENTS

The authors would like to acknowledge the financial assistance supported by the National Natural Science Foundation of China (grant No. 51273109).

REFERENCES

1. Sadasivuni, K. K.; Ponnamma, D.; Thomas, S.; Grohensa, Y. *Prog. Polym. Sci.* **2014**, *39*, 749.
2. Barrett, J. S. F.; Abdala, A. A.; Srienc, F. *Macromolecules* **2014**, *47*, 3926.
3. Kang, H.; Zuo, K.; Wang, Z.; Zhang, L.; Liu, L.; Guo, B. *Compos. Sci. Technol.* **2014**, *92*, 1.
4. Tang, Z.; Wu, X.; Guo, B.; Zhang, L.; Jia, D. *J. Mater. Chem.* **2012**, *22*, 7492.
5. Zhou, W.; Wang, X.; Wang, P.; Zhang, W.; Ji, J. *J. Appl. Polym. Sci.* **2013**, *130*, 4075.
6. Wang, Y.; Tsai, H. B. *J. Appl. Polym. Sci.* **2012**, *123*, 3154.
7. Yang, Z. Q.; Yuan, Y.; Li, F. L.; Liao, R. J. *J. Appl. Polym. Sci.* **2015**, *132*, 41385.
8. Bora, C.; Gogoi, P.; Baglari, S.; Dolui, S. K. *J. Appl. Polym. Sci.* **2013**, *129*, 3432.
9. Yoo, B. M.; Shin, H. J.; Yoon, H. W.; Park, H. B. *J. Appl. Polym. Sci.* **2014**, *131*, 39628.
10. Wei, J.; Qiu, J. *Polymer* **2014**, *55*, 3818.
11. Yang, J. H.; Shen, Y.; He, W. D.; Zhang, N.; Huang, T.; Zhang, J. H.; Wang, Y. *J. Appl. Polym. Sci.* **2013**, *130*, 3498.
12. Yan, N.; Xia, H.; Wu, J.; Zhan, Y.; Fei, G.; Chen, C. *J. Appl. Polym. Sci.* **2013**, *127*, 933.
13. Zhang, Y.; Mark, J. E.; Zhu, Y.; Ruoff, R. S.; Schaefer, D. W. *Polymer* **2014**, *55*, 5389.
14. Liu, X.; Kuang, W.; Guo, B. *Polymer* **2015**, *56*, 553.
15. Sarkawi, S. S.; Dierkes, W. K.; Noordermeer, J. W. M. *Eur. Polym. J.* **2013**, *49*, 3199.
16. Potts, J. R.; Shankar, O.; Du, L.; Ruoff, R. S. *Macromolecules* **2012**, *45*, 6045.
17. Sepehri, A.; Razzaghi-Kashani, M.; Ghoreishy, M. H. R. *J. Appl. Polym. Sci.* **2012**, *125*, E204.
18. Zhang, Y.; Zhu, W.; Lin, G.; Ruoff, R. S.; Hu, N.; Schaefer, D. W.; Mark, J. E. *Polymer* **2013**, *54*, 3605.
19. Bao, R. Y.; Liu, Z. Y.; Yang, W.; Xie, B. H.; Yang, M. B. *J. Mater. Chem. A* **2014**, *2*, 3190.
20. Cao, Y.; Feng, J.; Wu, P. *Carbon* **2010**, *48*, 1683.
21. Shanmugharaj, A. M.; Yoon, J. H.; Yang, W. J.; Ryu, S. H. *J. Colloid Interface Sci.* **2013**, *401*, 148.
22. Zhang, S. P.; Song, H. O. *New J. Chem.* **2012**, *36*, 1733.
23. Zhang, S.; Xiong, P.; Yang, X.; Wang, X. *Nanoscale* **2011**, *3*, 2169.
24. Choudhary, S.; Mungseand, H. P.; Khatri, O. P. *J. Mater. Chem.* **2012**, *22*, 21032.
25. Arabya, S.; Meng, Q.; Zhang, L.; Kang, H.; Majewski, P.; Tang, Y.; Ma, J. *Polymer* **2014**, *55*, 201.
26. Xiong, X.; Wang, J.; Jia, H.; Fang, E.; Ding, L. *Polym. Degrad. Stab.* **2013**, *98*, 2208.
27. Liang, J.; Huang, Y.; Zhang, L.; Wang, Y.; Ma, Y.; Guo, T.; Chen, Y. *Adv. Funct. Mater.* **2009**, *19*, 2297.
28. Wu, J.; Xing, W.; Huang, G.; Li, H.; Tang, M.; Wu, S.; Liu, Y. *Polymer* **2013**, *54*, 3314.
29. Araby, S.; Zhang, L.; Kuan, H. C.; Dai, J. B.; Majewski, P.; Ma, J. *Polymer* **2013**, *54*, 3663.
30. Heo, C.; Moon, H. G.; Yoon, C. S.; Chang, J. H. *J. Appl. Polym. Sci.* **2012**, *124*, 4663.
31. Wang, J.; Jia, H.; Tang, L.; Ji, Y.; Sun, D.; Gong, Y.; Ding, X. L. *J. Mater. Sci.* **2013**, *48*, 1571.
32. Tian, M.; Zhang, J.; Zhang, L.; Liu, S.; Zan, X.; Nishi, T.; Ning, N. *J. Colloid Interface Sci.* **2014**, *430*, 249.
33. Hu, H.; Zhao, L.; Liu, J.; Liu, Y.; Cheng, J.; Luo, J.; Liang, Y.; Tao, Y.; Wang, X.; Zhao, J. *Polymer* **2012**, *53*, 3378.
34. Kraus, G. *J. Appl. Polym. Sci.* **1963**, *7*, 861.
35. Yan, H.; Tian, G.; Sun, K.; Zhang, Y.; Zhang, Y. *J. Polym. Sci. Part B: Polym. Phys.* **2005**, *43*, 573.
36. Zhou, Y.; Wang, S.; Zhang, Y.; Zhang, Y. *J. Polym. Sci. Part B: Polym. Phys.* **2006**, *44*, 1226.
37. Fröhlich, J.; Niedermeier, W.; Luginsland, H. D. *Compos. Pt. A-Appl. Sci. Manuf.* **2005**, *36*, 449.
38. Kadlcak, J.; Kuritka, L.; Tunnicliffe, L. B.; Cermak, R. *J. Appl. Polym. Sci.* **2015**, *132*, 41976.
39. Payne, A. R. *J. Appl. Polym. Sci.* **1962**, *19*, 57.
40. Tang, Z.; Wei, Q.; Lin, T.; Guo, B.; Jia, D. *RSC Adv.* **2013**, *3*, 17057.
41. Subramaniam, K.; Das, A.; Steinhauser, D.; Klüppeland, M.; Heinrich, G. *Eur. Polym. J.* **2011**, *47*, 2234.
42. Krishnamoorti, R.; Ren, J.; Silva, A. S. *J Chem. Phys.* **2001**, *114*, 4968.
43. Feng, C.; Zhang, H.; Zhang, Y. *Polym. Compos.* **2014**, *35*, 2194.